Exact analytic solutions for a Dirac electron moving in graphene under magnetic fields



2009 J. Phys.: Condens. Matter 21 455305

(http://iopscience.iop.org/0953-8984/21/45/455305)

J. Phys.: Condens. Matter **21** (2009) 455305 (11pp) doi:10.1088/0953-8984/21/45/455305

# Exact analytic solutions for a Dirac electron moving in graphene under magnetic fields

**Ş Kuru**[1], **J Negro**[2] **and L M Nieto**[2]

[1] Department of Physics, Faculty of Science, Ankara University, 06100 Ankara, Turkey
[2] Departamento de Física Teórica, Atómica y Óptica, Universidad de Valladolid, E-47071 Valladolid, Spain

E-mail: sengul.kuru@science.ankara.edu.tr, jnegro@fta.uva.es and luismi@metodos.fam.cie.uva.es

Received 31 July 2009, in final form 11 September 2009
Published 23 October 2009
Online at stacks.iop.org/JPhysCM/21/455305

**Abstract**
Exact analytical solutions for the bound states of a graphene Dirac electron in various magnetic fields with translational symmetry are obtained. In order to solve the time-independent Dirac–Weyl equation the factorization method used in supersymmetric quantum mechanics is adapted to this problem. The behavior of the discrete spectrum, probability and current densities are discussed.

## 1. Introduction

The discovery of graphene [1, 2], a two-dimensional layer of graphite, and the massless Dirac character of the low energy electrons moving has attracted much interest in physics due to its important electronic properties. In particular, it is a scenario where some fundamental aspects of relativistic quantum mechanics can be addressed, such as the Klein–Gordon paradox or the anomalous Landau–Hall effect [2, 3]. Also, graphene is an appropriate material to develop electronic devices. Recently a series of studies concerning the interaction of graphene electrons in perpendicular magnetic fields (sometimes including electrostatic fields parallel to the layer surface) have been carried out in order to find a way for confining the charges [4–12]. In these works the Dirac–Weyl equation for massless electrons with a Fermi velocity $v_F$ is considered, where a minimal coupling with the vector potential describes the interaction with the external field. In general, some kinds of numerical computation were needed to find the energy levels of confined states or transmission coefficients for scattering states.

In this paper our interest is to consider interactions under perpendicular magnetic fields invariant under translations in one direction, and at the same time allowing for exact analytical solutions of the Dirac–Weyl equation. In order to achieve this goal we will adapt the factorization method and the techniques of supersymmetric quantum mechanics (SUSY-QM) to this situation [13–18]. This will allow us to gather here a number of problems where the results can be easily discussed, and at the same time we can interpret them in light of other situations previously considered in the literature. Let us mention that some SUSY-QM methods have been applied to graphene to obtain the exact and numerical solutions of Dirac electron Hamiltonians [19, 20] and also to describe the quantum Hall effect [21–23].

The organization of this paper is as follows. In section 2 we introduce the factorization method in the framework of the Dirac–Weyl equation for a massless electron in a magnetic field. Section 3 supplies a list of cases that can be solved using this method and with some figures describing basic properties. We end with some comments on the obtained results in section 4.

## 2. The Dirac–Weyl equation and SUSY partner Hamiltonians

In graphene a Dirac electron moves with an effective Fermi velocity $v_F = c/300$, where $c$ is the velocity of light, and behaves as a massless quasi-particle. The effective Hamiltonian around a Dirac point for a Dirac electron has the form [2]

$$H = v_F(\boldsymbol{\sigma} \cdot \mathbf{p}), \tag{2.1}$$

where $\boldsymbol{\sigma} = (\sigma_x, \sigma_y)$ are the Pauli matrices and $\mathbf{p} = -i\hbar(\partial_x, \partial_y)$ is the two-dimensional momentum operator. The

 

massless Dirac–Weyl equation in $(2+1)$ dimensions takes the form

$$v_{\mathrm{F}}(\boldsymbol{\sigma}\cdot\mathbf{p})\Phi(x,y,t)=\mathrm{i}\hbar\frac{\partial\Phi(x,y,t)}{\partial t}. \tag{2.2}$$

Here, we are interested in stationary states, thus substituting $\Phi(x,y,t)=\Psi(x,y)\mathrm{e}^{-\mathrm{i}Et/\hbar}$ into (2.2), we get the time-independent Dirac–Weyl equation

$$v_{\mathrm{F}}(\boldsymbol{\sigma}\cdot\mathbf{p})\Psi(x,y)=E\Psi(x,y). \tag{2.3}$$

The interaction of a Dirac electron with a magnetic field perpendicular to the graphene surface is described by (2.3), replacing the momentum operator $\mathbf{p}$ by $\mathbf{p}+e\mathbf{A}/c$, according to the minimal coupling rule, with $(-e)$ the charge of the electron, with the vector potential and the magnetic field given by

$$\mathbf{A}=(A_x,A_y,0),\qquad \mathbf{B}=\nabla\times\mathbf{A}. \tag{2.4}$$

Then, equation (2.3) becomes

$$v_{\mathrm{F}}\left[\boldsymbol{\sigma}\cdot\left(\mathbf{p}+\frac{e}{c}\mathbf{A}\right)\right]\Psi(x,y)=E\Psi(x,y). \tag{2.5}$$

The two-component wavefunction is the column matrix $\Psi(x,y)=(\phi_1(x,y),\phi_2(x,y))^{\mathrm{T}}$, with the super-index T denoting matrix transposition. From equation (2.5) we can write the two coupled equations for the components $\phi_1(x,y)$ and $\phi_2(x,y)$ as

$$-\mathrm{i}\left(\frac{\partial}{\partial x}+\mathrm{i}\frac{eA_x}{c\hbar}-\mathrm{i}\frac{\partial}{\partial y}+\frac{eA_y}{c\hbar}\right)\phi_2(x,y)=\mathcal{E}\phi_1(x,y) \tag{2.6}$$

$$-\mathrm{i}\left(\frac{\partial}{\partial x}+\mathrm{i}\frac{eA_x}{c\hbar}+\mathrm{i}\frac{\partial}{\partial y}-\frac{eA_y}{c\hbar}\right)\phi_1(x,y)=\mathcal{E}\phi_2(x,y), \tag{2.7}$$

where $\mathcal{E}=E/(\hbar v_{\mathrm{F}})$. In this paper we will focus on interactions with external magnetic fields having a translational symmetry along a direction in such a way that the problem can be solved analytically. We fix the symmetry direction as the $y$ axis and choose the Landau gauge for the vector potential so that

$$\mathbf{A}(x)=(0,A_y(x),0),\qquad \mathbf{B}=(0,0,B(x)),\qquad B(x)=\frac{\mathrm{d}A_y(x)}{\mathrm{d}x}. \tag{2.8}$$

By means of this gauge, equations (2.6) and (2.7) are independent of $y$, and therefore we can separate the wavefunction in the form $\Psi(x,y)=\mathrm{e}^{\mathrm{i}ky}(\psi_1(x),\mathrm{i}\psi_2(x))^{\mathrm{T}}$, where $k$ is the wavenumber in the $y$ direction. Then, equations (2.6) and (2.7) become

$$\left(\frac{\mathrm{d}}{\mathrm{d}x}+k+\frac{e}{c\hbar}A_y\right)\psi_2(x)=\mathcal{E}\psi_1(x), \tag{2.9}$$

$$\left(-\frac{\mathrm{d}}{\mathrm{d}x}+k+\frac{e}{c\hbar}A_y\right)\psi_1(x)=\mathcal{E}\psi_2(x). \tag{2.10}$$

The decoupled second-order differential equation satisfied by each component is

$$H_1\psi_1(x):=\left[-\frac{\mathrm{d}^2}{\mathrm{d}x^2}+\left(k+\frac{eA_y}{c\hbar}\right)^2+\frac{e}{c\hbar}\left(\frac{\mathrm{d}A_y}{\mathrm{d}x}\right)\right]\psi_1(x)=\varepsilon\psi_1(x), \tag{2.11}$$

$$H_2\psi_2(x):=\left[-\frac{\mathrm{d}^2}{\mathrm{d}x^2}+\left(k+\frac{eA_y}{c\hbar}\right)^2-\frac{e}{c\hbar}\left(\frac{\mathrm{d}A_y}{\mathrm{d}x}\right)\right]\psi_2(x)=\varepsilon\psi_2(x), \tag{2.12}$$

where

$$\varepsilon=\mathcal{E}^2=\frac{E^2}{\hbar^2v_{\mathrm{F}}^2}. \tag{2.13}$$

Therefore, we have arrived at two effective Hamiltonians in (2.11) and (2.12) for each component:

$$H_1=-\frac{\mathrm{d}^2}{\mathrm{d}x^2}+V_1(x),\qquad H_2=-\frac{\mathrm{d}^2}{\mathrm{d}x^2}+V_2(x), \tag{2.14}$$

which are interrelated by the Dirac–Weyl equation. Now, observe that if we define the first-order differential operators (adjoint of each other)

$$L^{\pm}=\mp\frac{\mathrm{d}}{\mathrm{d}x}+W(x), \tag{2.15}$$

where the superpotential function $W(x)$ is

$$W(x)=k+\frac{eA_y}{c\hbar}, \tag{2.16}$$

relations (2.9) and (2.10) can be rewritten in the form

$$L^-\psi_2(x)=\mathcal{E}\psi_1(x),\qquad L^+\psi_1(x)=\mathcal{E}\psi_2(x). \tag{2.17}$$

The Hamiltonians $H_1$ and $H_2$ are factorized as

$$H_1=L^-L^+,\qquad H_2=L^+L^- \tag{2.18}$$

and the effective potentials are expressed in the following way:

$$V_1=W^2+W',\qquad V_2=W^2-W', \tag{2.19}$$

where the prime denotes here differentiation with respect to $x$. From relations (2.17)–(2.19) we can state that the Hamiltonians $H_1$ and $H_2$ are one-dimensional supersymmetric partner Hamiltonians, linked by the intertwining (or SUSY) transformations $L^{\pm}$ [14]:

$$H_1L^-=L^-H_2,\qquad H_2L^+=L^+H_1. \tag{2.20}$$

There are many properties that can be inferred from this relation. In particular, if we assume that the spectrum of $H_1$ ($H_2$) is known, then its partner $H_2$ ($H_1$) will have the same spectrum except possibly the ground state (as is required from (2.11) and (2.12)). In order to fix some details, we will consider separately three characteristic cases of special physical interest.

(i) Let $\{\varepsilon_{2,n}\}$, $n = 0, 1, \ldots$, be the discrete spectrum of $H_2$ with corresponding real eigenfunctions $\{\psi_{2,n}\}$. If the ground state of $H_2$ is annihilated by $L^-$:

$$L^-\psi_{2,0} = 0, \tag{2.21}$$

then, from (2.18) the ground state eigenvalue of $H_2$ is $\varepsilon_{2,0} = 0$ and the discrete spectrum of $H_1$ will consist of the eigenvalues $\{\varepsilon_{1,n}\}$ and normalized eigenfunctions $\{\psi_{1,n}\}$ given by

$$\begin{aligned} \varepsilon_{1,n-1} &= \varepsilon_{2,n}, \\ \psi_{1,n-1}(x) &:= \frac{1}{\sqrt{\varepsilon_{2,n}}} L^-\psi_{2,n}(x), \qquad n = 1, 2, \ldots. \end{aligned} \tag{2.22}$$

Using our gauge, and taking into account the above results, we have that the eigenfunctions of the Dirac–Weyl equation (2.5), with the notation (2.13) for the energies, are

$$\begin{aligned} \mathcal{E}_0 &:= \varepsilon_{2,0} = 0, \\ \Psi_0(x, y) &= \mathrm{e}^{\mathrm{i}ky} \begin{pmatrix} 0 \\ \mathrm{i}\psi_{2,0}(x) \end{pmatrix}, \\ \mathcal{E}_{\pm,n} &:= \pm\sqrt{\varepsilon_{2,n}} = \pm\sqrt{\varepsilon_{1,n-1}}, \\ \Psi_n(x, y) &= \mathrm{e}^{\mathrm{i}ky} \begin{pmatrix} \psi_{1,n-1}(x) \\ \mathrm{i}\psi_{2,n}(x) \end{pmatrix}, \qquad n = 1, 2 \ldots. \end{aligned} \tag{2.23, 2.24}$$

In the following section we will take this as the standard case. Thus, we will give here two functions that are useful in studying the properties related to the states in the discrete spectrum (2.24): the probability density for an eigenfunction

$$\rho_n(x) = (\Psi_n)^\dagger \Psi_n = (\psi_{1,n-1}(x))^2 + (\psi_{2,n}(x))^2, \tag{2.25}$$

and the current density in the $y$ direction for this eigenfunction

$$j_n(x) = e v_\mathrm{F} (\Psi_n)^\dagger \sigma_y \Psi_n = 2e v_\mathrm{F} \psi_{1,n-1}(x)\psi_{2,n}(x). \tag{2.26}$$

In both cases the functions are constant in time, which corresponds to stationary states, and are independent of $y$, due to the translational symmetry.

Note that the discrete spectrum given by equations (2.23) and (2.24) has positive and negative eigenvalues disposed in a symmetric way. They correspond to electrons and holes, respectively.

(ii) A similar situation appears if we start with a known spectrum $\{\varepsilon_{1,n}\}$, $n = 0, 1, \ldots$ of $H_1$ with eigenfunctions $\{\psi_{1,n}\}$ and we suppose that

$$L^+\psi_{1,0} = 0. \tag{2.27}$$

Then, we would have $\varepsilon_{1,0} = 0$ and

$$\begin{aligned} \varepsilon_{2,n-1} &= \varepsilon_{1,n}, \\ \psi_{2,n-1}(x) &:= \frac{1}{\sqrt{\varepsilon_{1,n}}} L^+\psi_{1,n}(x), \qquad n = 1, 2 \ldots. \end{aligned} \tag{2.28}$$

with stationary solutions

$$\begin{aligned} \mathcal{E}_0 &:= \varepsilon_{1,0} = 0, \\ \Psi_0(x, y) &= \mathrm{e}^{\mathrm{i}ky} \begin{pmatrix} \psi_{1,0}(x) \\ 0 \end{pmatrix}, \\ \mathcal{E}_{\pm,n} &:= \pm\sqrt{\varepsilon_{1,n}} = \pm\sqrt{\varepsilon_{2,n-1}}, \\ \Psi_n(x, y) &= \mathrm{e}^{\mathrm{i}ky} \begin{pmatrix} \psi_{1,n}(x) \\ \mathrm{i}\psi_{2,n-1}(x) \end{pmatrix}, \qquad n = 1, 2, \ldots. \end{aligned} \tag{2.29, 2.30}$$

(iii) Still, there is a third situation that appears when the ground states of both partner Hamiltonians $H_1$ and $H_2$ have the same ground state eigenvalue (which must be different from zero). Then

$$L^+\psi_{1,0} \propto \psi_{2,0} \neq 0, \qquad L^-\psi_{2,0} \propto \psi_{1,0} \neq 0. \tag{2.31}$$

The eigenvalues of $H_1$ and $H_2$ are $\varepsilon_{1,n} = \varepsilon_{2,n} = \varepsilon_n$ and the component eigenfunctions

$$\begin{aligned} \psi_{1,n}(x) &:= \frac{1}{\sqrt{\varepsilon_n}} L^-\psi_{2,n}(x), \\ \psi_{2,n}(x) &= \frac{1}{\sqrt{\varepsilon_n}} L^+\psi_{1,n}(x). \end{aligned} \tag{2.32}$$

The spectrum of the Dirac–Weyl equation is

$$\begin{aligned} \mathcal{E}_{\pm,0} &:= \pm\sqrt{\varepsilon_0} \neq 0, \\ \mathcal{E}_{\pm,n} &:= \pm\sqrt{\varepsilon_n}, \qquad n = 1, 2, \ldots, \end{aligned} \tag{2.33}$$

and the corresponding two-component stationary eigenfunctions are

$$\Psi_n(x, y) = \mathrm{e}^{\mathrm{i}ky} \begin{pmatrix} \psi_{1,n}(x) \\ \mathrm{i}\psi_{2,n}(x) \end{pmatrix}, \qquad n = 0, 1, 2, \ldots. \tag{2.34}$$

## 3. Solvable cases

Now, we will analyze in detail some special cases of vector potentials that give rise to effective potentials whose exact analytic solutions can be found [13, 14]. We will pay special attention to the general common properties as well as to the main differences between these cases. Hereafter, we will assume (unless explicitly stated otherwise) that the involved parameters $\omega$, $\alpha$ and $D$ in the examples below are positive.

### *3.1. Case I: constant magnetic field*

From (2.8), in order to have a constant magnetic field perpendicular to the graphene plane in the positive direction of the $z$ axis, $\mathbf{B} = (0, 0, B_0)$, we can choose $A_y = B_0 x$. This is the very well-known case of Landau levels that has been considered in many references [2, 3]. In this case, the superpotential (2.16) is

$$W = k + \frac{eB_0}{c\hbar}x := k + \frac{1}{2}\omega x, \qquad B_0 = \frac{c\hbar}{2e}\omega, \tag{3.1}$$

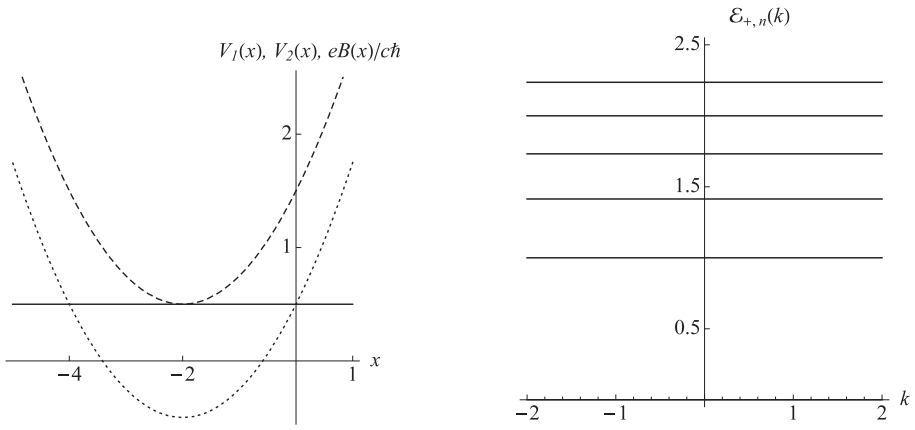


**Figure 1.** Constant field. On the left, plot of the effective potentials $V_1(x)$ (dashed line), $V_2(x)$ (dotted line) and the magnetic field $B(x) = 1/2$ (solid line) given in equations (3.1) and (3.2). The parameters are taken $\omega = k = 1$. Note that $V_1(x)$ and $B(x)$ touch at just one point: $x_0 = -2$, which coincides with the oscillator displacement. On the right, the first positive levels from equation (3.5), $\mathcal{E}_{+,0}(k), \ldots, \mathcal{E}_{+,5}(k)$ which, in the present case, are all constant.

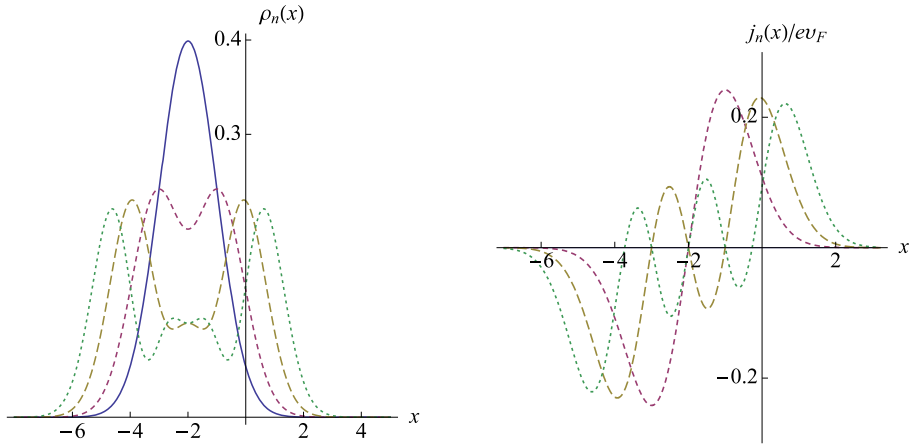


**Figure 2.** For a constant magnetic field $B(x) = 1/2$ and $\omega = k = 1$, on the left, plot of the density $\rho_n(x)$, for $n = 0, 1, 2, 3$ (the higher and more concentrated curve corresponds to $n = 0$, the lowest and more spread one corresponds to $n = 3$); on the right, plot of the current $j_n(x)/(ev_F)$, for $n = 1, 2$ and 3 (the styles are the same as the corresponding densities).

where we have introduced a constant $\omega$, whose dimensions are $(\text{length})^{-2}$. From (2.19), the super-partner potentials are the shifted oscillators:

$$V_1 = \frac{\omega^2}{4}\left(x + \frac{2k}{\omega}\right)^2 + \frac{1}{2}\omega, \qquad V_2 = \frac{\omega^2}{4}\left(x + \frac{2k}{\omega}\right)^2 - \frac{1}{2}\omega. \tag{3.2}$$

From here, obviously the eigenvalues for the corresponding partner Hamiltonians $H_1$ and $H_2$ are basically the same, but shifted one unit in $\omega$:

$$\varepsilon_{2,0} = 0, \qquad \varepsilon_{2,n} = \varepsilon_{1,n-1} = n\omega, \qquad n = 1, 2 \ldots. \tag{3.3}$$

The eigenfunctions are given in terms of Hermite polynomials, which corresponds to harmonic oscillator potentials:

$$\psi_{2,n}(z(x)) = \psi_{1,n}(z(x)) = C_n \mathrm{e}^{-\frac{1}{2}z^2} H_n(z) := \varphi_n(x), \qquad z = \sqrt{\frac{\omega}{2}}\left(x + \frac{2k}{\omega}\right), \tag{3.4}$$

where $C_n$ is a normalization constant. Then, taking into account (2.13), the eigenvalues of the Dirac–Weyl equation (2.5) are

$$\mathcal{E}_{\pm,n} = \pm\sqrt{\omega n}, \qquad n = 0, 1, \ldots. \tag{3.5}$$

The wavefunctions can be read from (2.24) as

$$\Psi_0(x, y) = \mathrm{e}^{\mathrm{i}ky}\begin{pmatrix} 0 \\ \mathrm{i}\varphi_0(x) \end{pmatrix}, \qquad \Psi_n(x, y) = \mathrm{e}^{\mathrm{i}ky}\begin{pmatrix} \varphi_{n-1}(x) \\ \mathrm{i}\varphi_n(x) \end{pmatrix}, \qquad n = 1, 2, \ldots. \tag{3.6}$$

Remark that the discrete spectrum (3.3) does not depend on the wavenumber $k$, which only affects the effective potentials (3.2) in a translation and the wavefunctions (3.6) in a global phase and in a displacement.

In figure 1 we show a plot of the effective potentials together with the magnetic field (left) and some of the first positive eigenvalues as functions of $k$ (right). We omit here, and in the next figures, the negative eigenvalues, which

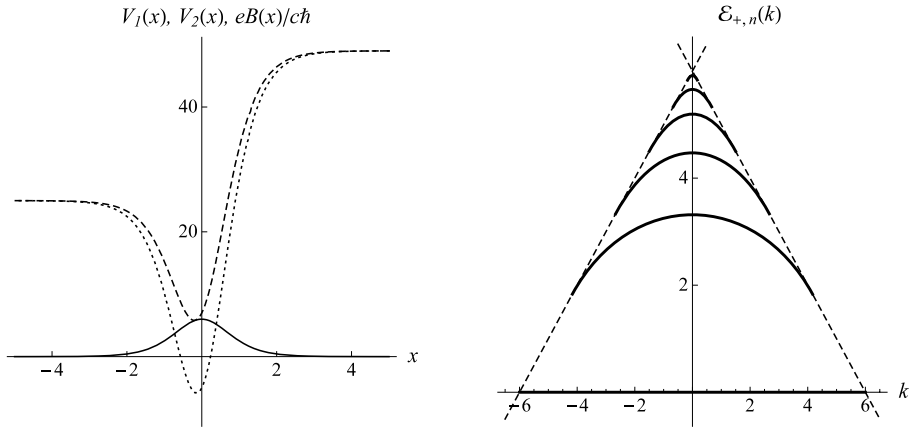


**Figure 3.** Hyperbolic well. Plot of the effective potentials $V_1$, $V_2$ and magnetic field $B$ given by (3.9) and (3.7), respectively (left) and the behavior of discrete energy levels $\mathcal{E}_{+,n}(k)$ depending on $k$ (right). We have chosen the first positive energy levels $\mathcal{E}_{+,0}(k), \ldots, \mathcal{E}_{+,n}(5)$. The parameters $\alpha = 1$, $D = 6$, $k = 1$ were taken for the left figure. As explained in the conclusions, $V_2$ and $eB/c\hbar$ touch at just one point and the energy levels have enveloping lines with slope $\pm v_F$.

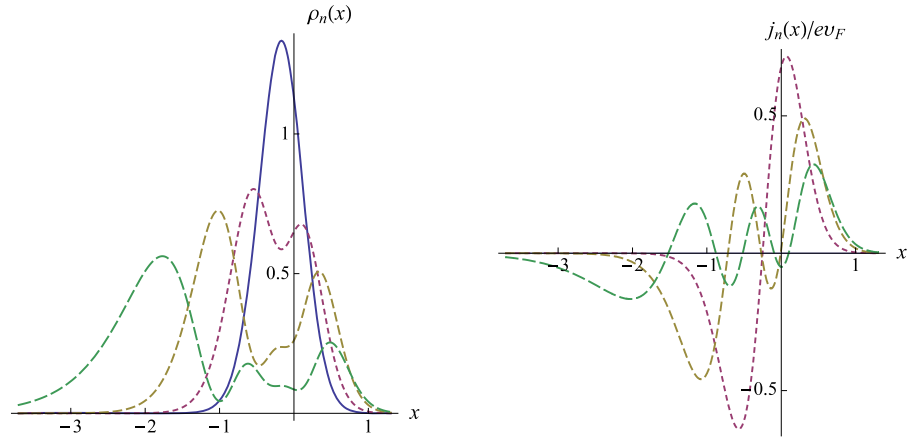


**Figure 4.** Plot of the density $\rho_n(x)$ for $n = 0, 1, 2, 3$ (left) and current $j_n(x)$ for $n = 1, 2, 3$ (right) in the case of an hyperbolic well. We have taken $\alpha = 1$, $D = 6$, $k = 1$. The style of corresponding probability and current densities are the same.

correspond to holes, and are completely symmetric to the positive ones, corresponding to electrons.

In figure 2 the density $\rho$ given by equation (2.25) and the current $j$ given by equation (2.26) are shown for some of the first eigenfunctions in (3.6).

With the above choice of parameters we were in the frame of case (i) of section 2. Had we taken the magnetic field in the direction of the negative $z$ axis, we would have obtained analogous solutions in the form of case (ii).

### *3.2. Case II: hyperbolic well or barrier*

Another interesting solvable case appears if we have a magnetic field with the following hyperbolic form:

$$\mathbf{B}(x) = \left(0, 0, \frac{B_0}{\cosh^2 \alpha x}\right). \tag{3.7}$$

From equation (2.8), the vector potential can be chosen to be $A_y = \frac{B_0}{\alpha} \tanh \alpha x$. Then, the superpotential is

$$W(x) = k + D \tanh \alpha x, \qquad D = \frac{eB_0}{\hbar c \alpha}, \tag{3.8}$$

and from (2.19) the super-partner potentials (sometimes called Rosen–Morse II potentials [13, 14]) are

$$V_1(x) = D^2 + k^2 - D(D - \alpha)\mathrm{sech}^2 \alpha x + 2kD \tanh \alpha x,$$
$$V_2(x) = D^2 + k^2 - D(D + \alpha)\mathrm{sech}^2 \alpha x + 2kD \tanh \alpha x. \tag{3.9}$$

Only if $k < D$ will the Hamiltonians $H_1$ and $H_2$ have a finite discrete spectrum whose eigenvalues are given by

$$\varepsilon_{2,n} = \varepsilon_{1,n-1} = D^2 + k^2 - (D - n\alpha)^2 - \frac{k^2 D^2}{(D - n\alpha)^2} > 0, \tag{3.10}$$

where $n = 0, 1, \ldots, N$, is such that $N\alpha < D < (N + 1)\alpha$. Taking $z = \tanh \alpha x$, $s_1 = \frac{D}{\alpha} - 1$, $s_2 = s_1 + 1$, $a_1 = \frac{kD}{\alpha(D - n\alpha + \alpha)}$ and $a_2 = \frac{kD}{\alpha(D - n\alpha)}$, the corresponding eigenfunctions are

$$\psi_{j,n}(z(x)) = (1 - z)^{(s_j - n + a_j)/2}(1 + z)^{(s_j - n - a_j)/2} \times P_n^{(s_j - n + a_j, s_j - n - a_j)}(z), \qquad j = 1, 2 \tag{3.11}$$

and $P_n^{(a,b)}(z)$ are Jacobi polynomials being $a, b > -1$. Remark that the exponents of the factors in (3.11) are greater than zero in order to satisfy the square-integrability condition.

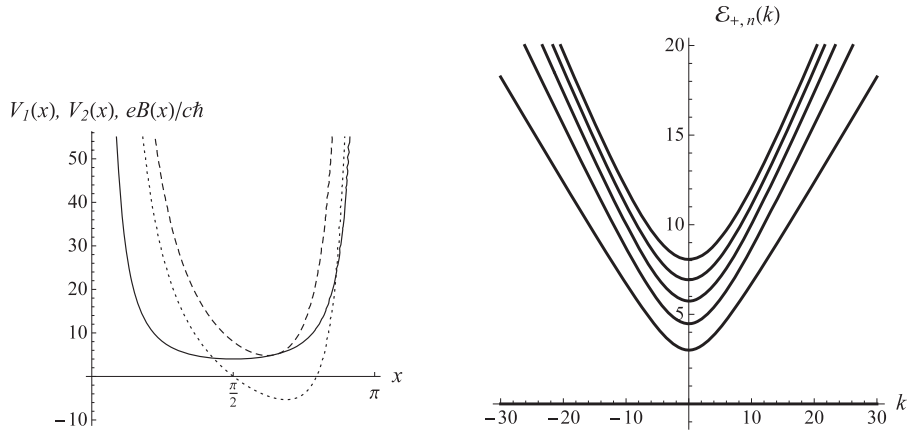


**Figure 5.** Trigonometric well. Plot of the effective potentials $V_1$, $V_2$ and magnetic field $B$ given by (3.15) and (3.13), respectively (left), and the first discrete energy levels $\mathcal{E}_{+,n}$ depending on $k$ given by (3.18) (right). The parameters $\alpha = 1$, $D = 4$, $k = -2$ were taken for the left figure.

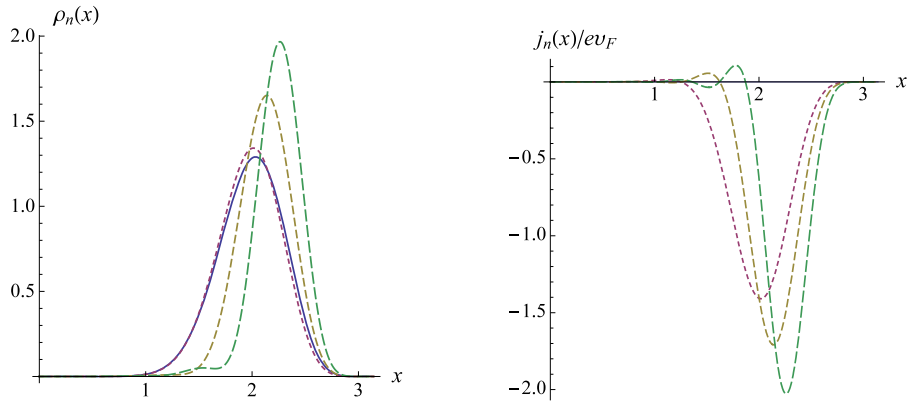


**Figure 6.** Plot of the density $\rho_n(x)$ for $n = 0, 1, 2, 3$ and current $j_n(x)$ for $n = 1, 2, 3$ in the case of a trigonometric well. We have taken $\alpha = 1$, $D = 4$, $k = -2$.

Then, the eigenfunctions of the Dirac–Weyl equation (2.5) can be read from equation (2.24) while the discrete eigenvalues are

$$\mathcal{E}_{\pm,n} = \pm\hbar v_F \sqrt{D^2 + k^2 - (D - n\alpha)^2 - \frac{k^2 D^2}{(D - n\alpha)^2}}. \quad (3.12)$$

As can be seen from the above formulae, the maximum number of discrete levels is determined exclusively by the quotient of the field parameters $D$ and $\alpha$. However, once $\alpha$ and $D$ fixed, as we increase $k$ (see figure 3, right) this number of levels decreases and at the same time the remaining levels have lower energies. In figure 3 we can see the plot of the effective potentials and magnetic field and the behavior of the spectrum as a function of the wavenumber $k$. Figure 4 displays the shape of the density $\rho_n$ and current $j_n$ for some bound states.

### *3.3. Case III: trigonometric singular well*

Let us consider now a magnetic field of trigonometric form, given by

$$\mathbf{B} = \left(0, 0, \frac{B_0}{\sin^2 \alpha x}\right), \qquad 0 \leqslant \alpha x \leqslant \pi. \quad (3.13)$$

In this case we are restricted to a strip $0 < x < \pi/\alpha$, such that in the borders the magnetic field diverges. This case represents a situation opposite to that of case II where the magnetic field was bigger at the center of the strip but vanished as $|x| \to \infty$. The vector potential is $A_y = -\frac{B_0}{\alpha}\cot\alpha x$, and the superpotential will be

$$W = k - D\cot\alpha x, \qquad D = \frac{eB_0}{\hbar c\alpha}. \quad (3.14)$$

The super-partner effective potentials (also called Rosen–Morse I potentials) from (2.19) have the form

$$\begin{aligned} V_1 &= k^2 - D^2 + D(D+\alpha)\mathrm{cosec}^2\alpha x - 2kD\cot\alpha x, \\ V_2 &= k^2 - D^2 + D(D-\alpha)\mathrm{cosec}^2\alpha x - 2kD\cot\alpha x. \end{aligned} \quad (3.15)$$

The corresponding eigenvalues, together with $\varepsilon_{2,0} = 0$, are

$$\varepsilon_{2,n} = \varepsilon_{2,n-1} = -D^2 + k^2 + (D + n\alpha)^2 - \frac{k^2 D^2}{(D + n\alpha)^2}, \quad (3.16)$$

and their eigenfunctions

$$\psi_{j,n}(z(x)) = (z^2 - 1)^{-(s_j+n)/2} \mathrm{e}^{a_j \alpha x} \times P_n^{(-s_j - n + \mathrm{i}a_j, -s_j - n - \mathrm{i}a_j)}(z), \qquad j = 1, 2 \quad (3.17)$$

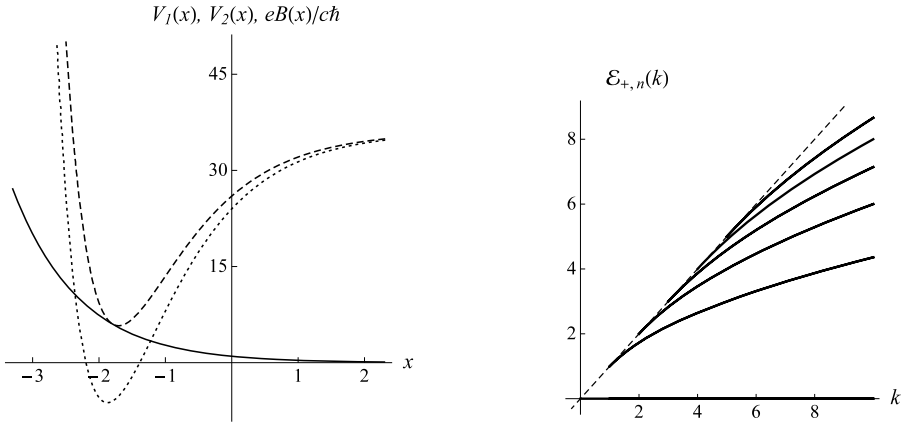


**Figure 7.** Exponential decaying field. Plot of the effective potentials $V_1$, $V_2$ and magnetic field $B$ given by (3.22) and (3.19), respectively (left) and the first discrete energy levels $\mathcal{E}_{+,n}(k)$, depending on $k$ (3.25) (right). The parameters $\alpha = 1$, $D = 1$, $k = 6$ were taken for the left figure.

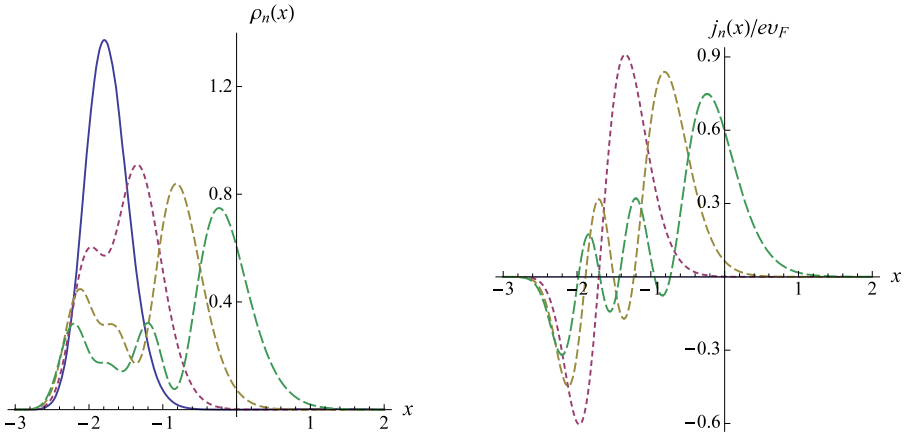


**Figure 8.** Plot of the density $\rho_n(x)$ for $n = 0, 1, 2, 3$ and current $j_n(x)$ for $n = 1, 2, 3$ in the case of a exponential decaying field. We have taken $\alpha = 1$, $D = 1$ and $k = 6$.

with $z = \mathrm{i}\cot\alpha x$, $s_2 = \frac{D}{\alpha}$, $a_2 = \frac{-kD}{\alpha(D+n\alpha)}$, $s_1 = s_2+1$ and $a_1 = \frac{-kD}{\alpha(D+n\alpha+\alpha)}$, where $P_n^{(a,b)}(z)$ are complex Jacobi polynomials. Another simpler expression for the solutions, avoiding Jacobi polynomials of complex arguments and parameters, is given in [24]. Then, the eigenvalues of (2.5) are

$$\mathcal{E}_{\pm,n} = \pm\sqrt{-D^2 + k^2 + (D+n\alpha)^2 - \frac{k^2D^2}{(D+n\alpha)^2}} \qquad (3.18)$$

and the eigenfunctions can be read from equation (2.24). In this case, the admissible $k$ values allowing for discrete energies are unrestricted in the real line. These systems possess an infinite discrete spectrum whose values are continuous increasing functions of the wavenumber $k$. This behavior is opposite to the one we had for the magnetic barrier of the previous case. Some features of this case are displayed in figures 5 and 6.

### *3.4. Case IV: exponential decaying magnetic field*

In this situation we have the perpendicular magnetic field exponentially decaying in the positive $x$ direction:

$$\mathbf{B} = (0, 0, B_0\mathrm{e}^{-\alpha x}). \qquad (3.19)$$

Now, the non-zero component of the vector potential is

$$A_y = -\frac{B_0}{\alpha}\mathrm{e}^{-\alpha x} \qquad (3.20)$$

and the superpotential is

$$W = k - D\mathrm{e}^{-\alpha x}, \qquad D = \frac{eB_0}{\hbar c\alpha}. \qquad (3.21)$$

Then, the partner potentials derived from (2.19) are just Morse potentials [14]:

$$\begin{aligned} V_1 &= k^2 + D^2\mathrm{e}^{-2\alpha x} - 2D\left(k - \frac{\alpha}{2}\right)\mathrm{e}^{-\alpha x}, \\ V_2 &= k^2 + D^2\mathrm{e}^{-2\alpha x} - 2D\left(k + \frac{\alpha}{2}\right)\mathrm{e}^{-\alpha x}. \end{aligned} \qquad (3.22)$$

The corresponding eigenvalues are

$$\varepsilon_{2,n} = \varepsilon_{1,n-1} = k^2 - (k - n\alpha)^2, \qquad (3.23)$$

and the component eigenfunctions are

$$\psi_{j,n}(z(x)) = z^{s_j-n}\mathrm{e}^{-z/2}L_n^{2s_j-2n}(z), \qquad j = 1, 2 \qquad (3.24)$$

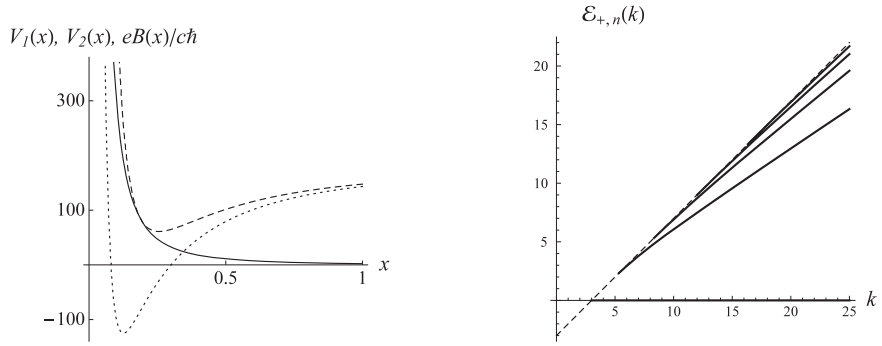


**Figure 9.** Singular hyperbolic field. Plot of the effective potentials $V_1$, $V_2$ and magnetic field $B$ according to (3.29) and (3.26), respectively (left), and the first discrete energy levels $\mathcal{E}_{+,n}(k)$ depending on $k$ given by (3.32) (right). The parameters $\alpha = 1$, $D = 3$ and $k = 16$ were taken for the left figure.

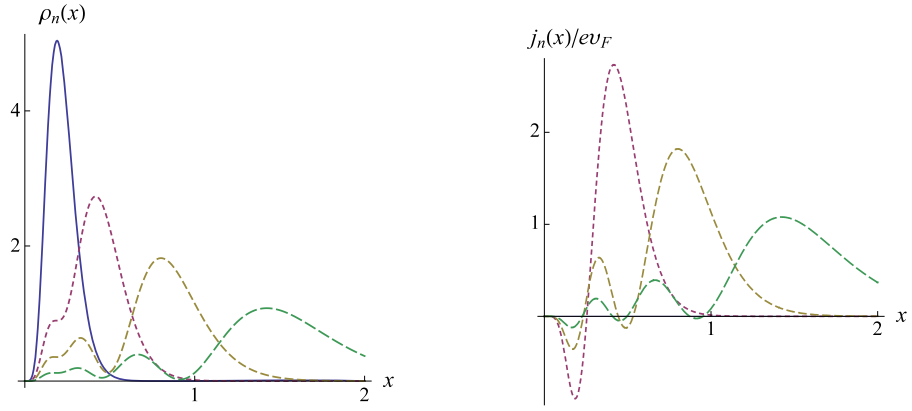


**Figure 10.** Plot of the density $\rho_n(x)$ for $n = 0, 1, 2, 3$ and current $j_n(x)$ for $n = 1, 2, 3$ in the case of a singular hyperbolic field. We have taken $\alpha = 1$, $D = 3$ and $k = 16$.

where $z = (\frac{2D}{\alpha})e^{-\alpha x}$, $s_2 = \frac{k}{\alpha}$, $s_1 = s_2 - 1$ and $L_n^{2s-2n}(z)$ are associated Laguerre polynomials with the condition $2s - 2n > -1$. At the same time, to guarantee square-integrability the condition $s - n > 0$ is necessary, due to the accompanying factors. Both conditions are satisfied when $k > \alpha n$. Thus, we have that the Dirac–Weyl two-component eigenfunctions take the form (2.24) of case (i) and the eigenvalues are

$$\mathcal{E}_{\pm,n} = \pm\sqrt{k^2 - (k - n\alpha)^2}. \tag{3.25}$$

These results, in our notation, are the same as those obtained in [11]. Remark that in this case the allowed energies as well as their number will depend on $k$. In fact the number of bound states will grow linearly with $k$. On the other hand, the coefficient $D$, giving the intensity of the magnetic field, does not affect the energy but only the wavefunctions as a displacement. If the exponential decay is in the opposite $x$ direction, then the formulae should be changed according to case (ii) of section 2. Some details of this case are given in figures 7 and 8.

### *3.5. Case V: hyperbolic singular field*

The magnetic field for this case is

$$\mathbf{B} = \left(0, 0, \frac{B_0}{\sinh^2 \alpha x}\right), \tag{3.26}$$

so that it diverges at one side of the strip $x = 0$ and exponentially vanishes as $x \to +\infty$ on the other side (figure 9). The corresponding vector potential is

$$A_y = -\frac{\hbar D}{e}\coth \alpha x, \tag{3.27}$$

leading to the superpotential

$$W = k - D\coth \alpha x, \qquad D = \frac{eB_0}{\hbar c\alpha}, \tag{3.28}$$

and the super-partner potentials (the so-called Eckart potentials) from (2.19) are

$$\begin{aligned} V_1 &= k^2 + D^2 + D(D+\alpha)\mathrm{cosech}^2\alpha x - 2kD\coth \alpha x, \\ V_2 &= k^2 + D^2 + D(D-\alpha)\mathrm{cosech}^2\alpha x - 2kD\coth \alpha x. \end{aligned} \tag{3.29}$$

In order to allow for bound states we must take $k > D$, the corresponding eigenvalues are given by $\varepsilon_{2,0} = 0$ and

$$\varepsilon_{2,n} = \varepsilon_{1,n-1} = D^2 + k^2 - (D + n\alpha)^2 - \frac{k^2D^2}{(D+n\alpha)^2}. \tag{3.30}$$

Their associated eigenfunctions take the form

$$\begin{aligned} \psi_{j,n}(z(x)) &= (z-1)^{-(s_j+n-a_j)/2}(z+1)^{-(s_j+n+a_j)/2} \\ &\times P_n^{(-s_j-n+a_j,-s_j-n-a_j)}(z), \qquad j = 1, 2 \end{aligned} \tag{3.31}$$

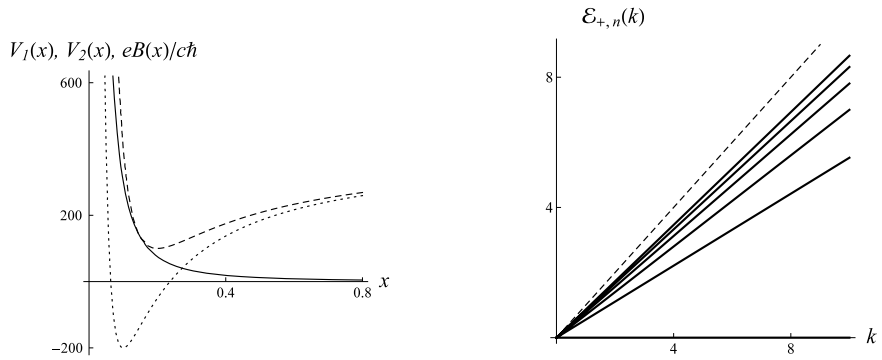


**Figure 11.** Singular field. Plot of the effective potentials $V_1$, $V_2$ and magnetic field $B$ according to (3.35) and (3.33), respectively (left), and the first discrete energy levels $\mathcal{E}_{+,n}(k)$ depending on $k$ fixed by (3.39) (right). The parameters $D = 3$, $k = 20$ were taken for the left figure. Note that, as always, $V_2$ and $B$ touch at just one point. The line $v_F = k$, shown in the figure, gives the limit of the slope of the bound state lines.

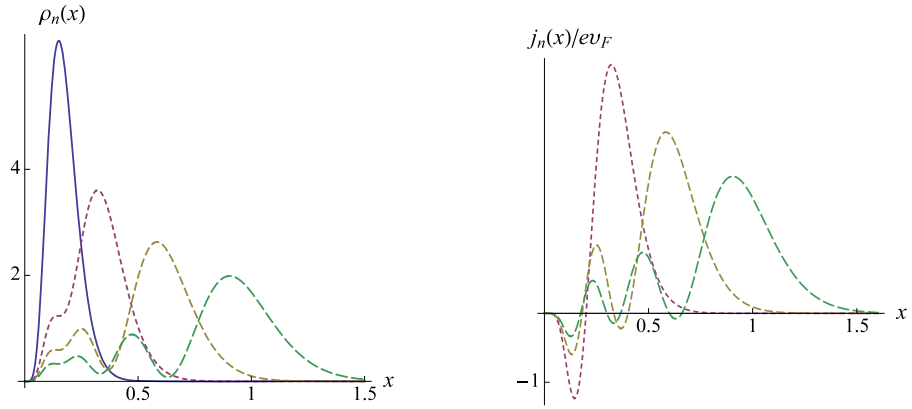


**Figure 12.** Plot of the density $\rho_n(x)$ for $n = 0, 1, 2, 3$ and current $j_n(x)$ for $n = 1, 2, 3$ in the case of a singular field. We have taken $D = 3$ and $k = 20$.

with $z = \coth \alpha x$, $s_2 = \frac{D}{\alpha}$, $a_2 = \frac{kD}{\alpha(D+n\alpha)}$, $s_1 = s_2 + 1$ and $a_1 = \frac{kD}{\alpha(D+n\alpha+\alpha)}$, where again $P_n^{(a,b)}(z)$ are Jacobi polynomials with $a, b > -1$. The square-integrability of the functions (3.31) is satisfied whenever $k > D$. Then, the eigenvalues of (2.5) are

$$\mathcal{E}_{\pm,n} = \pm\sqrt{D^2 + k^2 - (D + n\alpha)^2 - \frac{k^2 D^2}{(D + n\alpha)^2}} \qquad (3.32)$$

and the matrix eigenfunctions can be read according to equation (2.24). This case is similar to the previous one, where the discrete spectrum appears only if the wavenumber $k > 0$ (since, as said above, $k > D$) and the number of discrete levels depends on $k$. However, here the spectrum as well as the wavefunctions depend strongly on $D$ of the magnetic field. It can be seen from figure 9 that this is due to the behavior of the potential when $x$ tends to $+\infty$. The probability density $\rho_n(x)$ and the current density $j_n(x)$ are also plotted in figure 10.

### *3.6. Case VI: singular magnetic field*

The magnetic field for this case is

$$\mathbf{B} = \left(0, 0, \frac{B_0}{x^2}\right), \qquad (3.33)$$

whose vector potential is given by $A_y = -B_0/x$. We have a similar situation to the previous case: the system is defined in the half-line $(0, +\infty)$ where the field diverges in the origin but vanishes as $x \to +\infty$ (see figure 11). However, since the behavior in $x \to +\infty$ is rational, not exponential, it will lead to differences in the spectrum. Now, the superpotential is

$$W = k - \frac{D}{x}, \qquad D = \frac{eB_0}{\hbar c}, \qquad (3.34)$$

and the super-partner potentials (2.19) are radial Coulomb potentials with a centrifugal term:

$$\begin{aligned} V_1 &= k^2 + \frac{D(D+1)}{x^2} - \frac{2kD}{x}, \\ V_2 &= k^2 + \frac{D(D-1)}{x^2} - \frac{2kD}{x}, \qquad D > 1. \end{aligned} \qquad (3.35)$$

The eigenvalues of this problem are well known:

$$\varepsilon_2^{(n)} = \varepsilon_1^{(n-1)} = k^2 D^2 \left(\frac{1}{D^2} - \frac{1}{(n+D)^2}\right) \qquad (3.36)$$

while the eigenfunctions can be expressed in terms of Laguerre polynomials $L_n^a(x)$:

$$\psi_{1,n}(z_1(x)) = z_1^{D+1}\mathrm{e}^{-z_1/2}L_n^{2D+1}(z_1), \qquad z_1 = \frac{2kD}{n+D+1}x \tag{3.37}$$

and

$$\psi_{2,n}(z_2(x)) = z_2^{D}\mathrm{e}^{-z_2/2}L_n^{2D-1}(z_2), \qquad z_2 = \frac{2kD}{n+D}x. \tag{3.38}$$

The initial condition $D > 1$ guarantees the square-integrability of these eigenfunctions. Then, the eigenvalues of the Dirac–Weyl equation (2.5) are

$$\mathcal{E}_{\pm,n} = \pm kD\sqrt{\frac{1}{D^2} - \frac{1}{(n+D)^2}} \tag{3.39}$$

and their corresponding matrix eigenfunctions can be read as always from equation (2.24). As we said above this problem has similarities with case V, for instance, there will be no discrete spectrum unless the wavenumber $k$ is positive. However, once $k > 0$, due to the change of exponential by rational functions the number of levels is infinite and the value of $k$ affects their energy values linearly. For this case the plots of probability density $\rho_n(x)$ and current density $j_n(x)$ can be seen in figure 12.

## 4. Conclusions

In this paper we have studied some cases where the wavefunctions of electrons in a graphene layer under the influence of perpendicular magnetic fields can be found in an analytical closed form. Our aim is to show the relation between the massless Dirac–Weyl equation and SUSY quantum mechanics. We have used SUSY techniques in order to solve the Dirac–Weyl equation. In this way we have obtained six different cases that can be solved analytically. We have discussed the main features of these cases concerning the bound states that were illustrated in some figures.

Here, we want to make a remark on the $k$ values allowing for bound states. Due to the independence of the Hamiltonian on the $y$ variable, the canonical momentum $p_y$ must be a constant that we called $\hbar k$. Recall that, from a classical point of view, for a particle in a magnetic field with vector potential $\mathbf{A}$ (2.8) and charge $-e$, the $y$ component of momentum is $p_y = \pi_y - eA_y(x)/c$, where $\pi_y$ is interpreted as a 'kinematical' momentum in the $y$ direction. In other words, the quantity $\pi_y = \hbar k + eA_y(x)/c$ measures the motion in the $y$ direction.

Now, the value of $k$ fixed, consider a point $(x_0, y)$ of the plane in the line $x = x_0$, where $\pi_y(x_0) = \hbar k + eA_y(x_0)/c = 0$ and where $A_y(x)$ is monotonic (let us assume here that it is an increasing function). If we have our particle in a point $(x, y')$ with $x > x_0$, then $\pi_y = \hbar k + eA_y(x)/c > 0$. This means that the charge will move in the positive $y$ direction. However, when the particle is in a point with $x < x_0$ the kinematical momentum is negative and it will move in the opposite $y$ direction. For the points on the line where $x = x_0$, the motion in the $y$ direction vanishes and the particle can move only in the $x$ direction.

An example where this classical motion can happen is when the particle moves along a circle around the point $(x_0, y)$. We can assume that these conditions are also satisfied by other motions in the plane that enclose (maybe not by a circular trajectory, but by another kind of curve) each point $(x_0, y)$ of the $x_0$ line. If our picture is correct, such motions are close to the line $x = x_0$ and therefore they will characterize the bound states in the $x$ direction. We will see in the following that, in the cases under study, this conjecture is indeed correct for the bound states of our quantum systems. A more detailed discussion for more general cases will be given elsewhere.

Now we will look at the points $x_0$ where the kinematical momentum is zero. Notice that from our definition (2.16) of the superpotential $W(x)$ we have

$$W(x) = \hbar\pi_y(x)$$

and the field $B(x)$ in (2.8) is related to $W'(x)$ by

$$W'(x) = \frac{e}{c\hbar}B(x).$$

Therefore $W(x)$ and $W'(x)$ have a clear physical meaning. Let us take units where $\hbar = e/c\hbar = 1$ in order to simplify the expressions. For the effective potential $V_1$ (2.19) in the point $x_0$ where $W(x_0) = \pi_y(x_0) = 0$ we have

$$V_1(x_0) = W'(x_0) = B(x_0).$$

In other words, the point $x_0$ is characterized by the coincidence of the field $B$ and the partner potential $V_1$ using appropriate units. Since $V_1(x) = W(x)^2 + B(x)$, the effective potential $V_1$ is always greater than $B(x)$, except at $x_0$. This is shown in the figures displaying $V_1$, $V_2$ and $B$.

In the cases where $A_y(x)$ is increasing near $x_0$, as we discussed in the classical frame, for $x > x_0$ ($x < x_0$) then $\pi_y(x) > 0$ ($\pi_y(x) < 0$), so we expect that in the quantum case on these points we will have $j(x) > 0$ ($j(x) < 0$). This behavior is qualitatively appreciated in the plots of the current density $j_n(x)$. The fact that the line $x = x_0$ is related to the bound states is also shown in the figures of the density probability $\rho(x)$, especially for the ground state $\rho_0(x)$. We have checked in all the cases considered in this paper that the bound states take place only when the parameters of the potential and the wavenumber $k$ are such that there is a $x_0$ point where $W(x_0) = \pi_y(x_0) = 0$. However, we remark that we do not know if this property is satisfied in other cases.

A second feature is present in the figures representing the energies of bound states as a function of the wavenumber $k$. As mentioned above, these bound states correspond only to the motion in the $x$ direction, as a consequence of the separation of variables of the problem. However, as the problem is two-dimensional, the average velocity in the $y$ direction for these bound states can be computed as shown in [4, 8] in the form $v_n(k) = \partial E/\partial k$. As we have seen in figure 3 the bound states disappear as $k$ increases, but in figures 7 and 9 the bound states disappear as $k$ decreases. There are enveloping straight

lines with slope $\pm v_F$ touching the end points of these levels. This means that, at these points, where the states disappear as bound states and transform into scattering states, the average $y$ velocity is $\pm v_F$.

Essentially, we have dealt in this paper with two basic situations: (i) symmetric magnetic fields with respect to $x$ (cases I, II and III) and (ii) non-symmetric magnetic fields increasing towards one edge and vanishing in the opposite edge (cases IV, V and VI).

With respect to the symmetric case, it always allows for bound states for $k = 0$, while the spectrum will change as $k$ grows, except for the uniform field that can be considered as a reference that has the energy levels constant for any value of $k$. If we start with the constant value of the field at $x = 0$, we can modify the field, bending it downwards or upwards leading to cases II and III. We have seen that, in case II, where the field is bounded to the central region of the strip and vanishes at the edges, the spectrum values decreases as $|k|$ grows, and in this process the levels disappear one by one. However, in case III, where the magnetic field is very high on approaching both edges, the spectrum moves upward as $|k|$ increases.

As far as the second situation, we see that, due to the high values on one edge, and the vanishing on the other edge, it gives rise to a monotonic effective potential not allowing for bound states when $k = 0$. Only if $k \neq 0$ with the correct sign will we have an effective potential leading to bound states. This discrete spectrum, produced by $k$, will depend on the boundary behavior of the field.

## Acknowledgments

This work is partially supported by the Spanish MEC (FIS2009-09002 and MTM2009-10751), Junta de Castilla y León (GR 224) and Acción Complementaria FPA2008-04772-E/ARGEN. ŞK acknowledges the warm hospitality at the Department of Theoretical Physics, University of Valladolid, Spain.

## References

[1] Novoselov K S, Geim A K, Morozov S M, Zhang Y, Dubonos S V, Grigorieva I V and Firsov A A 2004 *Science* **306** 666
[2] Castro Neto A H, Guinea F, Peres N M, Novoselov K S and Geim A K 2009 *Rev. Mod. Phys.* **81** 109
[3] Gusynin V P and Sharapov S G 2008 *Phys. Rev. Lett.* **95** 146801
[4] Peeters F M and Matulis A 1993 *Phys. Rev.* B **48** 15166
[5] Milton Pereira J Jr, Mlinar V, Peeters F M and Vasilopoulos P 2006 *Phys. Rev.* B **74** 045424
[6] Lukose V, Shankar R and Baskaran G 2007 *Phys. Rev. Lett.* **98** 116802
[7] De Martino A, Dell'Anna L and Egger R 2007 *Phys. Rev. Lett.* **98** 066802
[8] Ramezani Masir M, Vasilopoulos P, Matulis A and Peeters F M 2008 *Phys. Rev.* B **77** 235443
[9] Ghosh T K, De Martino A, Häusler W, Dell'Anna L and Egger R 2008 *Phys. Rev.* B **77** 081404(R)
[10] Oroszlany L, Rakyta P, Kormanyos A, Lambert J C and Csertu J 2008 *Phys. Rev.* B **77** 081403(R)
[11] Ghosh T K 2009 *J. Phys.: Condens. Matter* **21** 045505
[12] Giavaras G, Maksym P A and Roy M 2009 *J. Phys.: Condens. Matter* **21** 102201
[13] Infeld L and Hull T E 1951 *Rev. Mod. Phys.* **23** 21
[14] Cooper F, Khare A and Sukhatme U 1995 *Phys. Rep.* **251** 267
[15] Fernández C D J, Negro J and del Olmo M A 1996 *Ann. Phys. NY* **252** 386
[16] Negro J, Nieto L M and Rosas-Ortiz O 2000 *J. Phys. A: Math. Gen.* **33** 7207
[17] Kuru Ş, Teğmen A and Verçin A 2001 *J. Math. Phys.* **42** 3344
[18] Demircioğlu B, Kuru Ş, Önder M and Verçin A 2002 *J. Math. Phys.* **43** 2133
[19] Setare M R and Hatami O 2008 *Chin. Phys. Lett.* **25** 3848
[20] Khmelnytskaya K V and Rosu H C 2009 *J. Phys. A: Math. Gen.* **42** 042004
[21] Ezawa M 2008 *Phys. Lett.* A **372** 924
[22] Ezawa M 2007 *Physique* E **40** 269
[23] Park K-S and Yi K S 2007 *J. Korean Phys. Soc.* **50** 1678
[24] Compean C B and Kirchbach M 2006 *J. Phys. A: Math. Gen.* **39** 547